



Published in final edited form as:

Int J Cancer. 2018 May 15; 142(10): 2153–2162. doi:10.1002/ijc.31234.

The sphingosine kinase 2 inhibitor ABC294640 displays anti-non-small cell lung cancer activities *in vitro* and *in vivo*

Lu Dai^{1,2}, Charles D. Smith³, Maryam Foroozesh⁴, Lucio Miele¹, and Zhiqiang Qin^{1,2,*}

¹Department of Genetics, Louisiana State University Health Sciences Center, Louisiana Cancer Research Center, 1700 Tulane Ave., New Orleans, LA 70112, USA

²Department of Pediatrics, Research Center for Translational Medicine and Key Laboratory of Arrhythmias, East Hospital, Tongji University School of Medicine, Shanghai 200120, China

³Apogee Biotechnology Corporation, Hummelstown, PA 17036, USA

⁴Department of Chemistry, Xavier University of Louisiana, 1 Drexel Drive, New Orleans, LA 70125, USA

Abstract

Non-small cell lung cancer (NSCLC) accounts for about 85–90% of lung cancer cases, and is the number one killer among cancers in the U.S. The majority of lung cancer patients do not respond well to conventional chemo- and/or radio-therapeutic regimens, and have a dismal 5-year survival rate of ~15%. The recent introduction of targeted therapy and immunotherapy gives new hopes to NSCLC patients, but even with these agents, not all patients respond, and responses are rarely complete. Thus, there is still an urgent need to identify new therapeutic targets in NSCLC and develop novel anti-cancer agents. Sphingosine kinase 2 (SphK2) is one of the key enzymes in sphingolipid metabolism. SphK2 expression predicts poor survival in NSCLC patients, and is associated with Gefitinib-resistance. In this study, the anti-NSCLC activities of ABC294640, the only first-in-class orally available inhibitor of SphK2, were explored. The results obtained indicate that ABC294640 treatment causes significant NSCLC cell apoptosis, cell cycle arrest, and suppression of tumor growth *in vitro* and *in vivo*. Moreover, lipidomics analyses revealed the complete signature of ceramide and dihydro(dh)-ceramide species in the NSCLC cell-lines with or without ABC294640 treatment. These findings indicate that sphingolipid metabolism targeted therapy may be developed as a promising strategy against NSCLC.

Keywords

NSCLC; sphingosine kinase; sphingolipid; ceramide

*Correspondence: Mailing address: Suite 902, Louisiana Cancer Research Center, 1700 Tulane Ave., New Orleans, LA 70112, USA. Phone: (504)-210-3327. zqin@lsuhsc.edu (Dr. Zhiqiang Qin).

Disclosure of Potential Conflicts of Interest

C.D. Smith is the President and Chief Executive Officer and has ownership interests (including patents) in Apogee Biotechnology Corporation. No potential conflicts of interest were disclosed by the other authors.

Introduction

Lung cancer is the number one killer among cancers in the United States with an estimated 155,870 deaths expected to occur in 2017.¹ It is also the second most diagnosed cancer in the U.S., and is responsible for approximate 222,500 new cases in 2017.¹ Based on histological features and cells of origin, lung cancers can be classified as small cell lung cancer (SCLC), a neuro-endocrine tumor, and non-small cell lung cancer (NSCLC), a group of epithelial-derived carcinomas including several sub-types. NSCLC accounts for about 85–90% of lung cancer cases. Clinically, the majority of lung cancer patients do not respond well to current chemo- and/or radio-therapeutic regimens, and have a very low 5-year survival rate of ~15%.² Recently, targeted therapy and immunotherapy have given new hopes to NSCLC patients, but the outcome/prognosis for most patients remains far from satisfactory. For instance, targeted therapeutic drugs such as Gefitinib that inhibits mutant epidermal growth factor receptor (EGFR), exhibit good initial effects. However, drug-resistance inevitably develops after 10 months of treatment, and patients eventually succumb to the disease.³ Inhibition of immune checkpoint receptors or ligands such as PD-1 and PD-L1 has yielded good clinical responses and improved overall survival in certain NSCLC patients, primarily in squamous carcinomas. However, only 15–20% of NSCLC patients respond to such therapy, and affordability is a serious issue, since a single-course (7-month) treatment will cost more than \$100,000.^{4,5} Thus, there is an urgent need to better understand the mechanisms of lung carcinogenesis and to identify new therapeutic targets to improve the treatment of NSCLC.

Sphingolipid biosynthesis involves the hydrolysis of ceramides to generate sphingosine, which is subsequently phosphorylated by one of two sphingosine kinase isoforms (SphK1 or SphK2) to generate sphingosine-1-phosphate (S1P).^{6,7} Bioactive sphingolipids including ceramides and S1P, can act as signaling molecules that regulate apoptosis and tumor cell survival.⁶ In contrast to the generally pro-apoptotic function of ceramides, S1P promotes cell proliferation and survival.⁷ S1P has been reported to promote the expansion of cancer stem cells through ligand-independent activation of Notch.⁸ Given the importance of SphKs in sphingolipid metabolism, a highly selective and well-characterized small molecule inhibitor of SphK2, ABC294640, has been recently developed,^{9,10} which displays significant anti-tumor activities for a variety of cancers such as lymphoma, prostate cancer, colorectal cancer, pancreatic cancer, and cholangiocarcinoma.^{11–15} However, there are limited data about the sphingolipid metabolism and targeted therapy in NSCLC. Johnson et al examined 25 NSCLC tumor samples and reported that they all overwhelmingly exhibited positive immunostaining for SphK1 as compared with patient-matched normal tissues.¹⁶ Wang et al reported that NSCLC patients with SphK2 overexpression in their tissues had lower overall survival (OS) and disease-free survival (DFS) rates than those with low SphK2 expression.¹⁷ Recently, Suzuki et al reported that combined treatment with 1- α -dimyristoylphosphatidylcholine liposome and the glucosylceramide synthase inhibitor D-PDMP induced NSCLC cell death associated with ceramide accumulation, and promoted cancer cell apoptosis and tumor regression in murine models.¹⁸ In general, there is still limited information on the lipidomics of ceramide species in NSCLC cells or sphingolipid metabolism targeted therapy for NSCLC. In this study, lipidomics analyses were performed

to identify the ceramide signature in NSCLC cell-lines with or without ABC294640 treatment. The anti-NSCLC activities of ABC294640 were also assessed *in vitro* and *in vivo*, and the underlying mechanisms were explored.

Materials and Methods

Cell culture and reagents

NSCLC cell lines (A549, H460, H1299) were kindly provided by Dr. Hua Lu at Tulane University, and cultured in RPMI-1640 medium supplemented with 10% fetal bovine serum and 1% penicillin & streptomycin. All experiments were carried out using cells harvested at low (<20) passages. 3-(4-chlorophenyl)-adamantane-1-carboxylic acid (pyridin-4-ylmethyl) amide (ABC294640) was synthesized as previously described.⁹ The pan-caspase inhibitor, Z-VAD-FMK, was purchased from Sigma (St. Louis, Missouri, USA).

Cell proliferation and apoptosis assays

Cell proliferation was measured using the WST-1 assays (Roche, Indianapolis, Indiana, USA) according to the manufacturer's instructions. Flow cytometry was used for quantitative assessment of apoptosis with the FITC-Annexin V/propidium iodide (PI) Apoptosis Detection Kit I (BD Pharmingen, San Jose, California, USA).

Cell cycle analysis

NSCLC cell pellets were fixed in 70% ethanol, and incubated at 4°C overnight. Cell pellets were re-suspended in 0.5 mL of 0.05 mg/mL PI plus 0.2 mg/mL RNaseA, and incubated at 37°C for 30 min. Cell cycle distribution was analyzed on a FACS Calibur 4-color flow cytometer (BD Bioscience, San Jose, California, USA).

RNA interference

For RNA interference (RNAi) assays, SphK2 ON-TARGETplus SMARTpool siRNA (Dharmacon, Lafayette, Colorado, USA), or negative control siRNA (n-siRNA), were delivered using the DharmaFECT transfection reagent according to the manufacturer's instructions.

Immunoblotting

Total cell lysates (20 µg) were resolved by 10% SDS-PAGE, transferred to nitrocellulose membranes, and immunoblotted with antibodies for SphK2, cleaved Caspase3/9, Myt1, phosphor-Cdc2, Cyclin B1, Cyclin D1, phosphor-Rb (Cell Signaling, Danvers, Massachusetts, USA) and β-Actin (Sigma, St. Louis, Missouri, USA) for loading controls. Immunoreactive bands were identified using an enhanced chemiluminescence reaction (Perkin-Elmer, Waltham, Massachusetts, USA), and visualized by autoradiography.

Quantitative real-time PCR

Total RNA was isolated using the RNeasy Mini kit (Qiagen, Germantown, Maryland, USA), and cDNA was synthesized from equivalent total RNA using a SuperScript III First-Strand Synthesis SuperMix Kit (Invitrogen, Waltham, Massachusetts, USA) according to the

manufacturer's instructions. Primers used for amplification of target genes are displayed in Table S1. Amplification was carried out using an iCycler IQ Real-Time PCR Detection System, and cycle threshold (*Ct*) values were tabulated in duplicate for each gene of interest in each experiment. "No template" (water) controls were used to ensure minimal background contamination. Using mean *Ct* values tabulated for each gene, and paired *Ct* values for β -actin as a loading control, fold changes for experimental groups relative to assigned controls were calculated using automated iQ5 2.0 software (Bio-Rad, Hercules, California, USA).

Spingolipid analyses

Quantification of sphingolipid species was performed using a Thermo Finnigan TSQ 7000 triple-stage quadrupole mass spectrometer operating in Multiple Reaction Monitoring positive ionization mode (Thermo Fisher Scientific, Waltham, Massachusetts, USA). Quantification was based on calibration curves generated by spiking an artificial matrix with known amounts of target standards and an equal amount of the internal standard. The target analyte:internal standard peak area ratios from each sample were compared with the calibration curves using linear regression. Final results were expressed as the ratio of sphingolipid normalized to total phospholipid phosphate level using the Bligh and Dyer lipid extract method.¹⁹

Nude mice xenograft models

Cells were counted and washed once in ice-cold PBS. 5×10^5 H460 cells in 50 μ L PBS plus 50 μ L growth factor-depleted Matrigel (BD Biosciences, San Jose, California, USA) were injected subcutaneously into the flank of nude mice (Jackson Laboratory, Sacramento, California, USA). Five days after this injection, the mice were randomly separated into two groups and received i.p. injection with either vehicle or ABC294640 (75 mg/kg of body weight dissolved in PEG:ddH₂O as 1:1), 3 days/week. The mice were observed and measured every 2–3 days for the presence of palpable tumors. At the end of the experiment, the tumors were excised for subsequent analyses. The animal experiments were repeated twice. All protocols were approved by the LSUHSC Animal Care and Use Committee in accordance with national guidelines.

Statistical analysis

Significance for differences between experimental and control groups was determined using the two-tailed Student's *t*-test (Excel 8.0), and *p* values <0.05 or <0.01 were considered significant or highly significant, respectively.

Results

Targeting SphK2 reduces NSCLC cell-lines proliferation in a dose-dependent manner

ABC294640 treatment alone was found to dramatically reduce the proliferation in NSCLC cell-lines (A549, H460, H1299) in a dose-dependent manner as determined by the WST-1 cell proliferation assays (Fig. 1). Notably, although H1299 cells have a homozygous partial deletion of p53 and mutant *NRAS*,²⁰ ABC294640 displayed similar efficacy among these three NSCLC cell-lines (IC₅₀ ranges 7.0–8.0 μ M). To further confirm the impact of targeting

SphK2 in the NSCLC cell proliferation, RNAi was used to directly silence SphK2, which also significantly reduced NSCLC cell-lines proliferation (Fig. S1).

Targeting SphK2 induces NSCLC cell cycle arrest and apoptosis

To further investigate the mechanisms through which ABC294640 reduces NSCLC cell proliferation, cell cycle distribution was analyzed by flow cytometry. It was found that ABC294640 treatment causes significant G2 phase arrest in all of the 3 NSCLC cell-lines tested (Fig. 2A). Subsequent immunoblot analyses indicated that ABC294640 regulates the expression of several cell cycle check-point factors, including the up-regulation of Myt1 and phospho-Cdc2, as well as the down-regulation of phosphor-Rb, Cyclin B1, and Cyclin D1 in A549 and H460 cells (Fig. 2B). Subsequent qRT-PCR analyses demonstrated that ABC294640 down-regulates Cyclin B1 and Cyclin D1 at the transcriptional level as well (Fig. S2). Furthermore, silencing SphK2 by RNAi also induced G2 cell cycle arrest in NSCLC cells, although at a lower extent than those caused by ABC294640 (Fig. S3).

ABC294640 treatment was found to cause apparent apoptosis in NSCLC cell-lines as detected by Annexin-V/PI staining and flow cytometry analysis (Fig. 3A). The data obtained indicated that ABC294640 induces a dose-dependent increase of cleaved caspase 3 and caspase 9 levels in A549 and H460 cells, while a pan-caspase inhibitor, Z-VAD-FMK (Z-VAD), almost completely protects NSCLC cells from the apoptosis induced by ABC294640 (Figs. 3B–C). In addition, silencing of SphK2 by RNAi caused significant cell apoptosis in A549 and H460 cell-lines (Fig. S4). Taken together, the results demonstrate that targeting SphK2 reduces NSCLC cell proliferation through inducing cell cycle arrest and caspase-dependent apoptosis.

ABC294640 increases the production of intracellular ceramides and dihydro(dh)-ceramides and alters their composition in NSCLC cells

Mass spectrometric-based lipidomics analyses were used to quantify intracellular levels of bioactive ceramide/dh-ceramide species in NSCLC cell-lines. It was observed that ABC294640 increases total levels of intracellular ceramides (1.5–3.5 folds) and dh-ceramides (3.0–7.5 folds) in the 3 NSCLC cell-lines tested (Fig. 4A). The lipidomics analyses of individual ceramide and dh-ceramide species indicated that most species including C14~C26-Cer and dhC14~dhC26-Cer were up-regulated in the 3 NSCLC cell-lines exposed to ABC294640, although the extent of the increases varies among these cell-lines (Figs. 4B–D). Since SphKs are responsible for phosphorylating sphingosine and generating S1P, it is not surprising to observe that ABC294640 treatment significantly reduces intracellular S1P levels and increases sphingosine levels in all the 3 NSCLC cell-lines (Fig. S5). Interestingly, a reduction of total sphingomyelin levels in NSCLC cell-lines exposed to ABC294640 was also observed (Fig. S6), implying that sphingomyelin hydrolysis²¹ may contribute to ABC294640-induced ceramides production.

The composition and proportion of individual ceramide and dh-ceramide species were calculated within the total lipid mass of NSCLC cell-lines with or without ABC294640 treatment (Figs. 5A–B). First, the top predominant ceramide/dh-ceramide species were identified within the NSCLC cell-lines studied, including C16-, C22-, C24:1-, C24-, dhC16-,

dhC18-, dhC22-, dhC24:1- and dhC24-Cer (Fig. 5C). Despite subtle differences, NSCLC cell-lines display a consistent ceramide signature. Second, it was found that ABC294640 treatment greatly alters the proportion of individual ceramide and dh-ceramide species within the NSCLC cell-lines studied (Fig. 5D). The most common proportional changes observed in all 3 NSCLC cell-lines include increased dhC22-Cer, and decreased C16-Cer and dhC16-Cer.

ABC294640 treatment effectively represses NSCLC tumor growth *in vivo*

By using an established H460 xenograft mice model, the effect of ABC294640 on NSCLC tumor growth was tested *in vivo*. H460 cells (5×10^5 cells, 1:1 with growth factor-depleted Matrigel) were injected subcutaneously into the flank of nude mice (5 mice per group). Five days after injection, the mice were randomly separated into two groups and received i.p. injections with either vehicle or ABC294640 (75 mg/kg of body weight), 3 days/week. The mice were observed every 2–3 days, and palpable tumors were measured over an additional 3 weeks. Results obtained indicate that ABC294640 treatment alone significantly represses tumor growth in mice compared to those observed in vehicle-treated mice (Fig. 6A). After the 3-week treatment period, the tumors isolated from ABC294640-treated mice had significantly smaller size than those from vehicle-treated mice (Fig. 6B). Immunoblot analyses confirmed increased expression of cleaved caspase 3 and caspase 9, and reduced expression of Cyclin B1 within tumor tissues from representative ABC294640-treated mice when compared to those from the vehicle-treated mice (Fig. 6C). Lipidomics analyses indicated that many ceramide and dh-ceramide species were up-regulated in tumor tissues of the ABC294640-treated mice when compared to those of the vehicle-treated mice (Figs. 6D–E), although the extents of these increases and sphingolipids patterns were subtly different from what we observed *in vitro*.

Discussion

There are three major pathways of ceramide generation: the sphingomyelinase pathway (sphingomyelin→ceramide); the *de novo* pathway (3-keto-dihydrosphingosine→dihydrosphingosine→dihydroceramide→ceramide); and the salvage pathway (S1P→sphingosine→ceramide).^{22,23} ABC294640, a selective inhibitor of SphK2 (an enzyme responsible for phosphorylating sphingosine and generating S1P), significantly reduces intracellular S1P levels and increases sphingosine levels in NSCLC cell-lines, through blocking the salvage pathway. ABC294640 treatment also greatly reduces the total levels of sphingomyelin, implying that the *de novo* pathway and sphingomyelinase pathway are also indirectly affected by ABC294640 in NSCLC cell-lines (Fig. 7). Our group is currently determining which ceramide synthases (CerSs, the key enzymes for ceramide generation in both the *de novo* pathway and the salvage pathway) and/or sphingomyelinases (SMases, the key enzymes for ceramide generation in the sphingomyelinase pathway) are responsible for ABC294640-induced ceramide production in NSCLC cells. At present, six different CerSs have been identified, CerS1–6,²⁴ and different isoforms of CerS generate an array of ceramide species with distinct chain lengths of fatty acids.²⁵ Previous data have shown that ABC294640 treatment increases the levels of several CerSs in a virus-associated lymphoma *in vitro* and *in vivo*.²⁶ The SMases are divided into acidic, neutral, and alkaline

forms dependent on their pH optimum.²⁷ For example, acidic SMase is localized in the lysosomal compartment and can also be secreted in the extracellular space.²⁸ Neutral SMase is present in the plasma membrane, cytoplasm, and the nucleus.²¹ In this study, it was also found that ABC294640 treatment increases a variety of dihydroceramides production in NSCLC cells. Interestingly, recent data have shown that ABC294640 can also inhibit dihydroceramide desaturase activity, resulting in the accumulation of dihydroceramides in prostate cancer cells, which is dispensable with SphK2 expression.^{12,29}

Here, it is reported that ABC294640 treatment can induce significant caspase-dependent apoptosis in NSCLC cells, which is closely related to increased intracellular production of ceramides. In fact, published reports have shown that ceramides can activate protein phosphatase 2A (PP2A) directly by binding inhibitor 2 of PP2A (I2PP2A/SET), thereby reducing the association between PP2A and its inhibitors.^{30,31} The effect of ceramides on PP2A leads to inactivation of Akt through dephosphorylation. In addition, apoptosis signal-regulating kinase 1 (Ask1) is a member of the mitogen-activated protein kinase kinase kinase (MAPKKK) family, which can be activated by ceramide, and initiates apoptosis.³² Our results have previously shown that ABC294640 treatment can affect the activities of the Akt and MAPK pathways in a virus-associated lymphoma.¹¹ Mitochondrial outer membrane permeabilization (MOMP) is a critical step in apoptosis. Ceramide is considered to be the main substance that induces MOMP, which is a key event in apoptotic signaling through the formation of ceramide channels to facilitate the passage of proteins released during MOMP.³³ Ganesan et al have indicated that ceramides are the key permeabilizing entity, and that Bax and ceramides can synergistically generate MOMP.³⁴ Ceramides can also contribute to MOMP by inducing the translocation to the mitochondria and activation of protein kinase C δ (PKC δ), which in turn promotes caspase 9 activation and cytochrome c release.³⁵ Further studies will determine which of these mechanisms is most prominent for the pro-apoptotic activity of ABC294640 in NSCLC cells.

The study reported here only focuses on single-agent ABC294640 treatment of NSCLC cells. A recent study reports that ABC294640 combined with tumor necrosis factor-related apoptosis-inducing ligand (TRAIL) can enhance the apoptosis of NSCLC cells.³⁶ Another recent study reports that inhibition of ceramide glucosylation by either a glucosylceramide synthase (GCS) inhibitor or GCS shRNA/siRNA knockdown can enhance ABC294640-induced NSCLC cell apoptosis.³⁷ Li and Zhang have summarized recent studies on combinations of chemotherapeutic drugs and ceramide-generating agents (e.g., CerS or SMase inducers) or modulators of ceramide metabolism (e.g., GCS or SphK inhibitors).²⁷ Generally, ceramide inducers sensitize cancer cells to anticancer agents resulting in enhanced cell apoptosis and death.²⁷ Very recently, Britten et al have reported promising results from a Phase I Study of ABC294640 in patients with advanced solid tumors.³⁸ They found that at 500 mg bid, ABC294640 was well tolerated and achieves biologically relevant plasma concentrations. These data together with the findings reported here indicate that sphingolipid metabolism targeted therapy may have broad prospects for clinical applications in oncology. An important question to be addressed is whether these agents target cancer stem-like cells, which are typically resistant to standard of care chemotherapy and are thought to be responsible for relapse and metastasis in many malignancies including lung cancer.

Supplementary Material

Refer to Web version on PubMed Central for supplementary material.

Acknowledgments

We thank Drs. Charles Chalfant and Jeremy Allegood at the Virginia Commonwealth University Lipidomics Core Facility for their assistance with sphingolipid analyses supported by NIH P30-CA016059 and a shared resource grant S1ORR031535. We also thank Dr. Hua Lu at Tulane University for kindly providing the NSCLC cell-lines. This work was supported by grants from a DOD Career Development Award to (CA140437 to Z. Qin), a Louisiana Clinical and Translational Science Center Pilot grant (U54GM104940 from NIH), a LSU LIFT² funding and NIH P20-GM121288-01 (PI: Krzysztof Reiss) subproject to Z. Qin, and the awards from the National Natural Science Foundation of China (81472547, 81672924 to Z. Qin and 81400164, 81772930 to L. Dai). The M. Foroozesh group acknowledges the funding by the DoD Breast Cancer grant (W81XWH-11-1-0105), the NIH awards TL4GM118968, R25GM060926, G12MD007595, and the Louisiana Cancer Research Center. Funding sources had no role in study design, data collection and analysis, decision to publish, or preparation of the manuscript.

References

1. American Cancer Society. Cancer Facts & Figures 2017. Atlanta: American Cancer Society; 2017.
2. Molina JR, Yang P, Cassivi SD, Schild SE, Adjei AA. Non-small cell lung cancer: epidemiology, risk factors, treatment, and survivorship. *Mayo Clinic Proc.* 2008; 83:584–94.
3. Ware KE, Hinz TK, Kleczko E, Singleton KR, Marek LA, Helfrich BA, Cummings CT, Graham DK, Astling D, Tan AC, Heasley LE. A mechanism of resistance to gefitinib mediated by cellular reprogramming and the acquisition of an FGF2-FGFR1 autocrine growth loop. *Oncogenesis.* 2013; 2:e39. [PubMed: 23552882]
4. Sundar R, Cho BC, Brahmer JR, Soo RA. Nivolumab in NSCLC: latest evidence and clinical potential. *Ther Adv Med Oncol.* 2015; 7:85–96. [PubMed: 25755681]
5. Andrews A. Treating with Checkpoint Inhibitors-Figure \$1 Million per Patient. *Am Health Drug Benefits.* 2015; 8:9. [PubMed: 26380599]
6. Ogretmen B, Hannun YA. Biologically active sphingolipids in cancer pathogenesis and treatment. *Nat Rev Cancer.* 2004; 4:604–16. [PubMed: 15286740]
7. Takabe K, Paugh SW, Milstien S, Spiegel S. “Inside-out” signaling of sphingosine-1-phosphate: therapeutic targets. *Pharmacol Rev.* 2008; 60:181–95. [PubMed: 18552276]
8. Hirata N, Yamada S, Shoda T, Kurihara M, Sekino Y, Kanda Y. Sphingosine-1-phosphate promotes expansion of cancer stem cells via S1PR3 by a ligand-independent Notch activation. *Nat Commun.* 2014; 5:4806. [PubMed: 25254944]
9. French KJ, Schrecengost RS, Lee BD, Zhuang Y, Smith SN, Eberly JL, Yun JK, Smith CD. Discovery and evaluation of inhibitors of human sphingosine kinase. *Cancer Res.* 2003; 63:5962–9. [PubMed: 14522923]
10. French KJ, Zhuang Y, Maines LW, Gao P, Wang W, Beljanski V, Upson JJ, Green CL, Keller SN, Smith CD. Pharmacology and antitumor activity of ABC294640, a selective inhibitor of sphingosine kinase-2. *J Pharmacol Exp Ther.* 2010; 333:129–39. [PubMed: 20061445]
11. Qin Z, Dai L, Trillo-Tinoco J, Senkal C, Wang W, Reske T, Bonstaff K, Del Valle L, Rodriguez P, Flemington E, Voelkel-Johnson C, Smith CD, et al. Targeting Sphingosine Kinase Induces Apoptosis and Tumor Regression for KSHV-Associated Primary Effusion Lymphoma. *Mol Cancer Ther.* 2014; 13:154–64. [PubMed: 24140934]
12. Venant H, Rahmaniyan M, Jones EE, Lu P, Lilly MB, Garrett-Mayer E, Drake RR, Kravka JM, Smith CD, Voelkel-Johnson C. The Sphingosine Kinase 2 Inhibitor ABC294640 Reduces the Growth of Prostate Cancer Cells and Results in Accumulation of Dihydroceramides In Vitro and In Vivo. *Mol Cancer Ther.* 2015; 14:2744–52. [PubMed: 26494858]
13. Xun C, Chen MB, Qi L, Tie-Ning Z, Peng X, Ning L, Zhi-Xiao C, Li-Wei W. Targeting sphingosine kinase 2 (SphK2) by ABC294640 inhibits colorectal cancer cell growth in vitro and in vivo. *J Exp Clin Cancer Res.* 2015; 34:94. [PubMed: 26337959]

14. Lewis CS, Voelkel-Johnson C, Smith CD. Suppression of c-Myc and RRM2 expression in pancreatic cancer cells by the sphingosine kinase-2 inhibitor ABC294640. *Oncotarget*. 2016; 7:60181–92. [PubMed: 27517489]
15. Ding X, Chaiteerakij R, Moser CD, Shaleh H, Boakye J, Chen G, Ndzengue A, Li Y, Zhou Y, Huang S, Sinicrope FA, Zou X, et al. Antitumor effect of the novel sphingosine kinase 2 inhibitor ABC294640 is enhanced by inhibition of autophagy and by sorafenib in human cholangiocarcinoma cells. *Oncotarget*. 2016; 7:20080–92. [PubMed: 26956050]
16. Johnson KR, Johnson KY, Crellin HG, Ogretmen B, Boylan AM, Harley RA, Obeid LM. Immunohistochemical distribution of sphingosine kinase 1 in normal and tumor lung tissue. *J Histochem Cytochem*. 2005; 53:1159–66. [PubMed: 15923363]
17. Wang Q, Li J, Li G, Li Y, Xu C, Li M, Xu G, Fu S. Prognostic significance of sphingosine kinase 2 expression in non-small cell lung cancer. *Tumor Biol*. 2014; 35:363–8.
18. Suzuki M, Cao K, Kato S, Komizu Y, Mizutani N, Tanaka K, Arima C, Tai MC, Yanagisawa K, Togawa N, Shiraishi T, Usami N, et al. Targeting ceramide synthase 6-dependent metastasis-prone phenotype in lung cancer cells. *J Clin Invest*. 2016; 126:254–65. [PubMed: 26650179]
19. Bielawski J, Szulc ZM, Hannun YA, Bielawska A. Simultaneous quantitative analysis of bioactive sphingolipids by high-performance liquid chromatography-tandem mass spectrometry. *Methods*. 2006; 39:82–91. [PubMed: 16828308]
20. Phelps RM, Johnson BE, Ihde DC, Gazdar AF, Carbone DP, McClintock PR, Linnoila RI, Matthews MJ, Bunn PA Jr, Carney D, Minna JD, Mulshine JL. NCI-Navy Medical Oncology Branch cell line data base. *J Cell Biochem Suppl*. 1996; 24:32–91. [PubMed: 8806092]
21. Huwiler A, Zangemeister-Wittke U. Targeting the conversion of ceramide to sphingosine 1-phosphate as a novel strategy for cancer therapy. *Crit Rev Oncol Hematol*. 2007; 63:150–9. [PubMed: 17560117]
22. Liu J, Beckman BS, Foroozesh M. A review of ceramide analogs as potential anticancer agents. *Future Med Chem*. 2013; 5:1405–21. [PubMed: 23919551]
23. Hannun YA, Obeid LM. Principles of bioactive lipid signaling: lessons from sphingolipids. *Nat Rev Mol Cell Biol*. 2008; 9:139–50. [PubMed: 18216770]
24. Stiban J, Tidhar R, Futerman AH. Ceramide synthases: roles in cell physiology and signaling. *Adv Exp Med Biol*. 2010; 688:60–71. [PubMed: 20919646]
25. Hannun YA, Obeid LM. Many ceramides. *J Biol Chem*. 2011; 286:27855–62. [PubMed: 21693702]
26. Dai L, Trillo-Tinoco J, Bai A, Chen Y, Bielawski J, Del Valle L, Smith CD, Ochoa AC, Qin Z, Parsons C. Ceramides promote apoptosis for virus-infected lymphoma cells through induction of ceramide synthases and viral lytic gene expression. *Oncotarget*. 2015; 6:24246–60. [PubMed: 26327294]
27. Li F, Zhang N. Ceramide: Therapeutic Potential in Combination Therapy for Cancer Treatment. *Curr Drug Metab*. 2015; 17:37–51. [PubMed: 26526831]
28. Aureli M, Murdica V, Loberto N, Samarani M, Prinetti A, Bassi R, Sonnino S. Exploring the link between ceramide and ionizing radiation. *Glycoconj J*. 2014; 31:449–59. [PubMed: 25129488]
29. McNaughton M, Pitman M, Pitson SM, Pyne NJ, Pyne S. Proteasomal degradation of sphingosine kinase 1 and inhibition of dihydroceramide desaturase by the sphingosine kinase inhibitors, SKi or ABC294640, induces growth arrest in androgen-independent LNCaP-AI prostate cancer cells. *Oncotarget*. 2016; 7:16663–75. [PubMed: 26934645]
30. Mukhopadhyay A, Saddoughi SA, Song P, Sultan I, Ponnusamy S, Senkal CE, Snook CF, Arnold HK, Sears RC, Hannun YA, Ogretmen B. Direct interaction between the inhibitor 2 and ceramide via sphingolipid-protein binding is involved in the regulation of protein phosphatase 2A activity and signaling. *FASEB J*. 2009; 23:751–63. [PubMed: 19028839]
31. Oaks J, Ogretmen B. Regulation of PP2A by Sphingolipid Metabolism and Signaling. *Front Oncol*. 2014; 4:388. [PubMed: 25642418]
32. Chen CL, Lin CF, Chang WT, Huang WC, Teng CF, Lin YS. Ceramide induces p38 MAPK and JNK activation through a mechanism involving a thioredoxin-interacting protein-mediated pathway. *Blood*. 2008; 111:4365–74. [PubMed: 18270325]

33. Chang KT, Anishkin A, Patwardhan GA, Beverly LJ, Siskind LJ, Colombini M. Ceramide channels: destabilization by Bcl-xL and role in apoptosis. *Biochem Biophys Acta*. 2015; 1848:2374–84. [PubMed: 26215742]
34. Ganesan V, Perera MN, Colombini D, Datskovskiy D, Chadha K, Colombini M. Ceramide and activated Bax act synergistically to permeabilize the mitochondrial outer membrane. *Apoptosis*. 2010; 15:553–62. [PubMed: 20101465]
35. Sumitomo M, Ohba M, Asakuma J, Asano T, Kuroki T, Asano T, Hayakawa M. Protein kinase Cdelta amplifies ceramide formation via mitochondrial signaling in prostate cancer cells. *J Clin Invest*. 2002; 109:827–36. [PubMed: 11901191]
36. Yang J, Yang C, Zhang S, Mei Z, Shi M, Sun S, Shi L, Wang Z, Wang Y, Li Z, Xie C. ABC294640, a sphingosine kinase 2 inhibitor, enhances the antitumor effects of TRAIL in non-small cell lung cancer. *Cancer Biol Ther*. 2015; 16:1194–204. [PubMed: 26054751]
37. Guan S, Liu YY, Yan T, Zhou J. Inhibition of ceramide glucosylation sensitizes lung cancer cells to ABC294640, a first-in-class small molecule SphK2 inhibitor. *Biochem Biophys Res Commun*. 2016; 476:230–6. [PubMed: 27221045]
38. Britten CD, Garrett-Mayer E, Chin SH, Shirai K, Ogretmen B, Bentz TA, Brisendine A, Anderton K, Cusack SL, Maines LW, Zhuang Y, Smith CD, et al. A Phase I Study of ABC294640, a First-in-Class Sphingosine Kinase-2 Inhibitor, in Patients with Advanced Solid Tumors. *Clin Cancer Res*. 2017; 23:4642–50. [PubMed: 28420720]

Novelty & Impact Statements

Therapy-resistance and poor survival in non-small cell lung cancer (NSCLC) are associated with expression of sphingosine kinase 2 (SphK2), an enzyme involved in sphingolipid metabolism. Anti-tumor activity via SphK2 inhibition with the small molecule ABC294640 has been observed, though the data are limited for NSCLC. Here, in NSCLC cell lines and a mouse xenograft model, ABC294640 treatment was shown to be associated with tumor cell apoptosis, cell cycle arrest, and reduced tumor growth. In NSCLC cells, ABC294640 treatment resulted in increased levels of bioactive sphingolipids, specifically ceramides and dihydro(dh)-ceramides. The data indicate that ABC294640 exerts significant anti-NSCLC activity *in vitro* and *in vivo*.

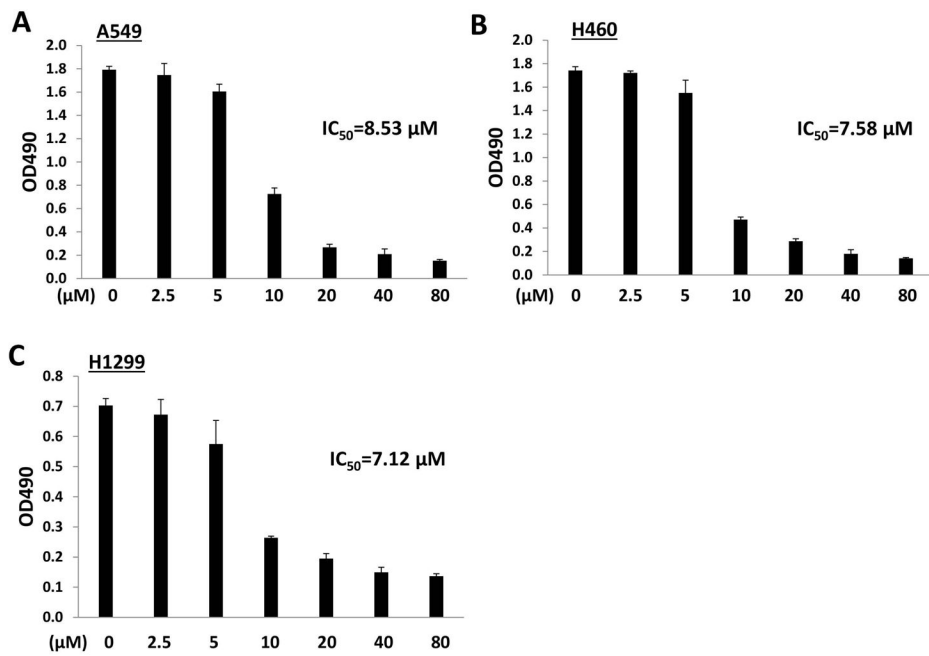


Figure 1. ABC294640 treatment represses the proliferation of NSCLC cell-lines
 (A–C) NSCLC cell-lines A549, H460, and H1299 were incubated with the indicated concentrations of ABC294640 (ABC) for 72 h; cell proliferation was measured using the WST-1 assays. Error bars represent the S.D. from 3 independent experiments. The 50% Inhibitory Concentration (IC_{50}) was calculated using SPSS 20.0 (Armonk, New York, USA).

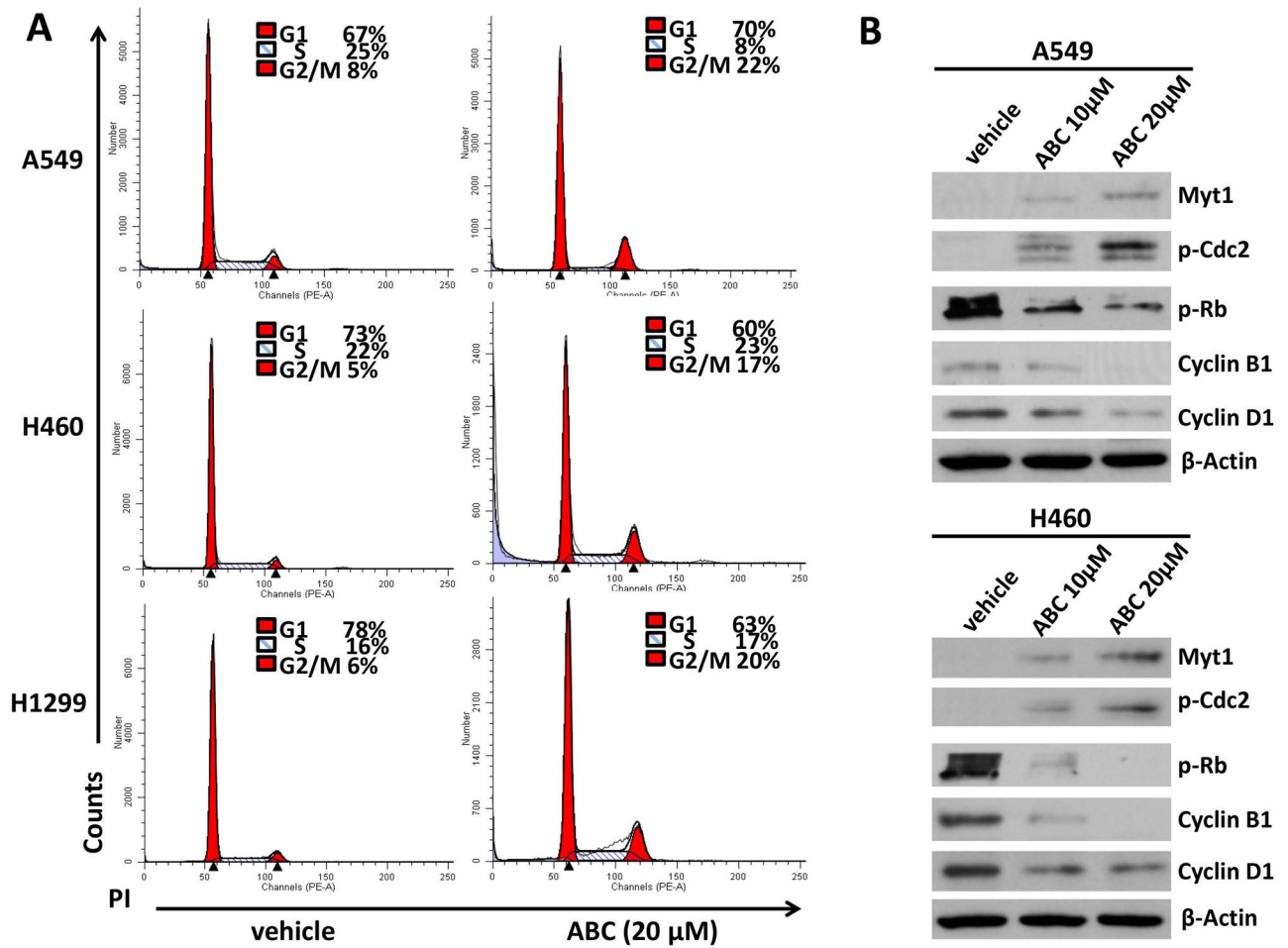


Figure 2. ABC294640 treatment causes NSCLC cell-lines G2 cell cycle arrest
(A–B) NSCLC cell-lines A549, H460, and H1299 were incubated with 10 or 20 μM of ABC294640 (ABC) or vehicle for 48 h, then stained by propidium iodide (PI), and analyzed by flow cytometry. Protein expression was analyzed by immunoblot analysis. The experiments were repeated twice, and one representative experiment results were shown.

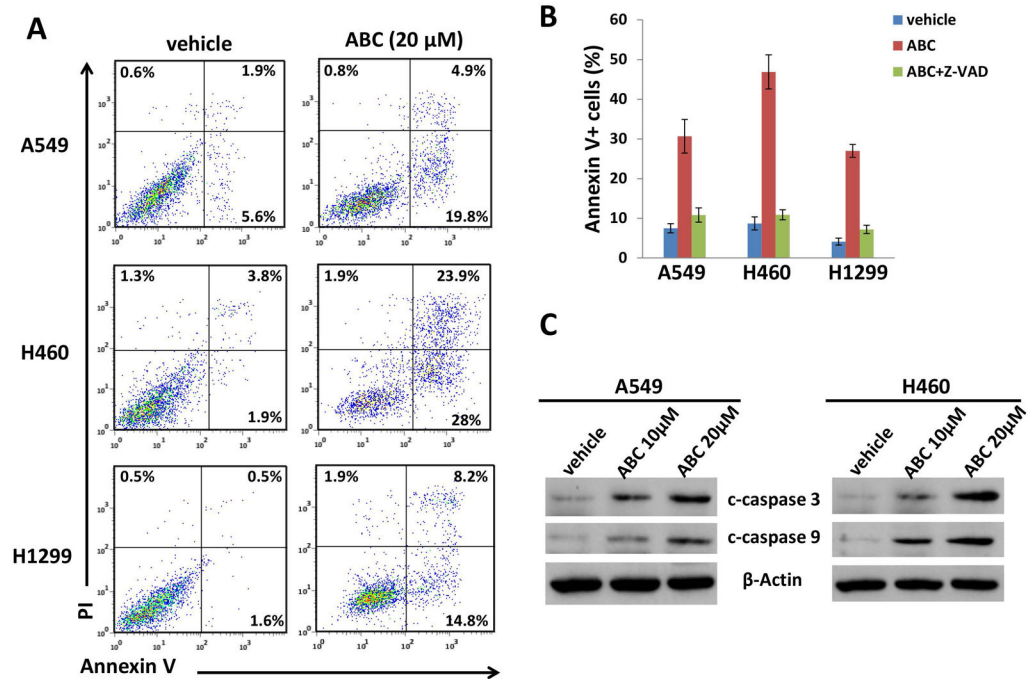


Figure 3. ABC294640 treatment induces NSCLC cell-lines apoptosis

(A–B) NSCLC cell-lines A549, H460, and H1299 were incubated with 20 μM of ABC294640 (ABC) or vehicle in the presence or absence of the pan-caspase inhibitor Z-VAD-FMK (Z-VAD, 10 μM) for 48 h; cell apoptosis was measured using Annexin V-PI staining and flow cytometry analysis. Error bars represent the S.D. from 3 independent experiments. (C) NSCLC cell-lines were incubated with 10 or 20 μM of ABC294640 (ABC) or vehicle for 48 h; protein expression was analyzed using immunoblot analysis.

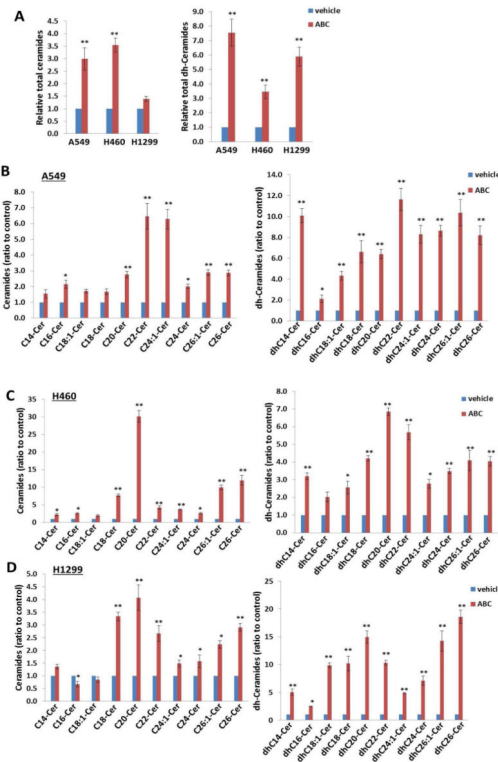


Figure 4. ABC294640 treatment induces intracellular ceramides production from NSCLC cell-lines

(A–D) NSCLC cell-lines A549, H460, and H1299 were incubated with vehicle or 20 μ M of ABC294640 (ABC) for 48 h; ceramide and dihydro(dh)-ceramide species were quantified using lipidomics analysis as described in the Methods. Error bars represent the S.D. from 3 independent experiments. * = $p < 0.05$, ** = $p < 0.01$.

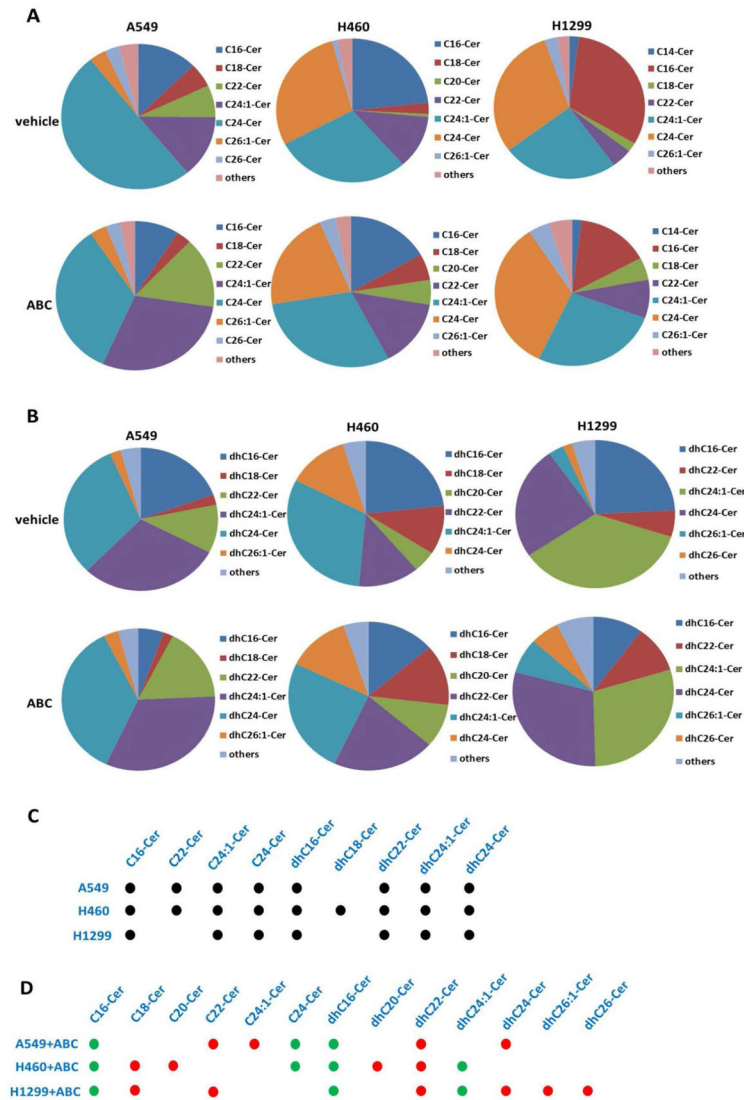


Figure 5. The compositions and proportions of ceramide/dh-ceramide species in NSCLC cell-lines are altered by ABC294640
 (A–B) Relative compositions and proportions of specific ceramide and dh-ceramide species present within vehicle- or ABC-treated NSCLC cell-lines are shown. Each color is representing a specific ceramide species and is labeled beside the pie chart. (C–D) Black dots represent the top prominent ceramide/dh-ceramide species present in NSCLC cell-lines. Red and green dots represent up-regulated or down-regulated ceramide/dh-ceramide species in NSCLC cell-lines exposed to ABC, respectively.

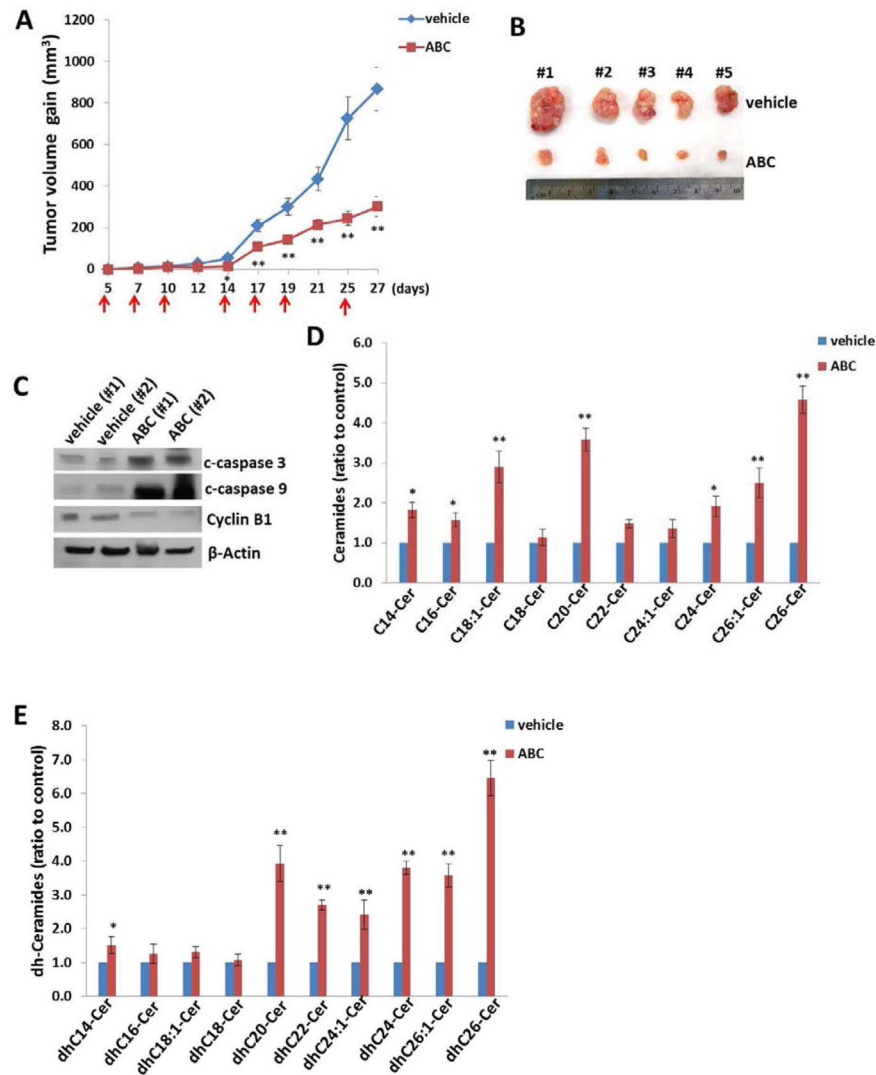


Figure 6. ABC294640 treatment effectively represses NSCLC growth *in vivo*

(A–B) NSCLC H460 cells (5×10^5 cells, 1:1 with growth factor-depleted Matrigel) were injected subcutaneously into the flank of nude mice. Five days after this injection, the mice were randomly separated into two groups and received i.p. injection with either vehicle or ABC294640 (75 mg/kg of body weight), 3 days/week. The arrows indicate the time points when ABC294640 or vehicle was administered. The mice were observed and measured every 2–3 days for the size of palpable tumors over an additional 3 weeks. At the end of the experiment, the tumors were excised for subsequent analyses. The numbers 1–5 represent different mice from the same group. Error bars represent the S.D. from one of the 2 independent experiments. (C–E) Protein expression in tumor tissues from representative mice was measured using immunoblots. The ceramide and dihydro(dh)-ceramide species within tumor tissues were quantified using lipidomics analysis as described in the Methods. Error bars represent the S.D. from 3 mice from each group. * = $p < 0.05$, ** = $p < 0.01$.

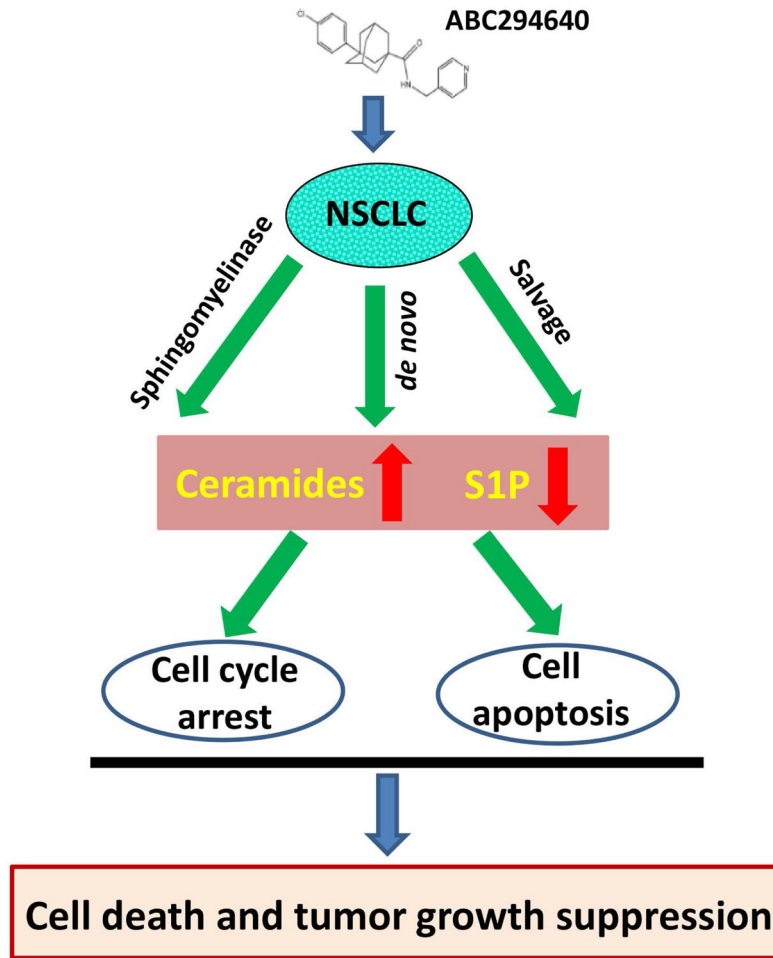


Figure 7. Schematic diagram of the possible mechanisms for anti-NSCLC activities of ABC294640.